

Thermal exposure to a steel column from localized fires

J. Sjöström, A. Byström, D. Lange and U. Wickström



Thermal exposure to a steel column from localized fires

Johan Sjöström, Alexandra Byström
David Lange, Ulf Wickström

Abstract

This study investigates the thermal exposure to a full scale steel column exposed to localized fires. The steel column is a six meters long cylinder with a diameter of 200 mm. The fires are heptane and diesel fires from cylindrical pans of diameter 1.1 m and one diesel fire using a pan of 1.9 m in diameter. The main result is the experimental data on gas and steel temperatures. All experimental data can be found on the SP website http://www.sp.se/en/index/services/localized_fire/sidor/default.aspx and in the Appendix of this report. A comparison to calculations using the Eurocode recommendations for localized fires is also conducted. Even when using assumptions to keep the thermal exposure to the structure at a low level the Eurocode calculations greatly overestimate the thermal exposure. We also conduct finite element calculations using plate thermometer measurements as input and describe the temperature evolution in the column considering the heat exchange within the hollow column.

The project is a collaboration between SP Fire Technology and Luleå Technical University. It is fully financed by Brandforsk, the Swedish Fire Research Board.

Key words: Thermal exposure, localized fire, steel column, plate thermometers, Eurocode

SP Sveriges Tekniska Forskningsinstitut
SP Technical Research Institute of Sweden

SP Report 2012:04
ISBN 978-91-87017-21-6
ISSN 0284-5172
Borås 2013

Contents

Abstract	3
Innehållsförteckning / Contents	4
1 Introduction	5
1.1 Heat transfer from flames	5
1.2 Previous work	6
2 Experiments	7
3 Results	9
3.1 Results from experiments	9
3.2 Comparison with Eurocode calculations	13
3.3 FEM calculations	16
4 Summary and conclusions	18
5 References	19
Appendix A – Instrumentation	20
Column and setup	20
Instrumentation	21
Appendix B – Results	27
Diesel fire $\varnothing=1.9$ m	27
Heptane fire $\varnothing=1.1$ m	30
Diesel fire $\varnothing=1.1$ m	32
Appendix C – Thermal action according to EN 1991-1-2	36
Appendix D –The Adiabatic Surface Temperature (AST) and plate thermometers	38
Appendix E –The effect of internal heat transfer	40

1 Introduction

In large in-door enclosures like airport terminals a fully developed fire with high uniform temperatures is unlikely. Still, an intense fire could locally expose structures to severe thermal conditions although the mean temperature in the enclosure is low. Usually structures are designed to resist the standard fire according to ISO 834 or EN 1363-1 for a specified time. Alternatively, parametric fires as specified in the Eurocode 1 (EN 1991-1-2 - Annex A) could be applied but all these design fires are intended for, and derived for, relatively small compartments where flashover with very high and uniform temperatures can develop. In large compartments we may instead anticipate localized fires, as specified in EN 1991-1-2 - Annex C, to consider high intensity fire exposure effects. The thermal exposure of such fires depends then not only on the flame temperature but also on the magnitude and dimensions of the flames as the thermal exposure is dominated by the irradiance level. Thus the exposure level could be relatively small despite high local fire gas temperatures. Furthermore, only parts of a structural element will be affected that may reduce the structural effects on load-bearing elements in comparison to a uniform exposure. Asymmetric fires may on the other hand make the exposure more severe due to e.g. buckling of columns. More detailed analyses allow for design according to more relevant thermal exposure levels as well as distributions along structures. Thus over design of fire protection measures could be avoided while still maintaining highly reliable and safe solutions.

To be able to design for non-flashover fires there is a need for experimental data on real scale structures exposed to localised fires. Very little such data are available in the literature. This work summarizes full-scale experiments on a steel column exposed to various pool fires in a large room.

For design purposes details on thermal impact from localized fire can be determined according to Eurocode 1 Appendix C. These are based to a large extent on plume theories [2, 3] mainly developed and evaluated for determinations of mass flow rates, plume temperature and flame heights and not so much for thermal exposures on structural elements. In this report the results of calculations based on Eurocode are compared with experimental data.

1.1 Heat transfer from flames

The heat transfer from the flame and hot gases to a surface consists of three main components, absorbed radiation, emitted radiation and convective heat transfer.

$$\dot{q}''_{tot} = \dot{q}''_{abs} - \dot{q}''_{emi} + \dot{q}''_{con} \quad (1)$$

Normally in fire sciences surface emissivity (absorptivity) is taken to be wavelength independent and the absorbed radiant heat flux is simply a portion of the incident radiant heat flux. This portion is determined by the surface emissivity, i.e. $\dot{q}''_{abs} = \epsilon_s \dot{q}''_{inc}$. The incident radiation, \dot{q}''_{inc} , depends on flame temperature, the view angle between flames and surface (Φ) and the flame emissivity.

The emitted radiation, \dot{q}''_{emi} , is determined by the surface temperature and the surface emissivity only:

$$\dot{q}''_{emi} = \epsilon_s \sigma T_s^4 \quad (2)$$

Convective heat transfer is generally assumed to be linear with respect to the difference between the surface- and gas temperatures. The proportionality constant is called the convective heat transfer coefficient, h_c :

$$\dot{q}''_{con} = h_c(T_g - T_s) \quad (3)$$

For adjacent fires the gas temperature is assumed to be equal to the temperature of the flames and the hot gases T_{fl} . Thus, the total heat transfer to a surface exposed to a localized fire can therefore be expressed as:

$$\dot{q}''_{tot} = \varepsilon_s \sigma (\Phi \varepsilon_{fl} T_{fl}^4 - T_s^4) + h_c (T_{fl} - T_s) \quad (4)$$

The flame emissivity is taken to be an exponentially dependent on the flame thickness as:

$$\varepsilon_{fl} = 1 - e^{-KL}, \quad (5)$$

where K is the absorption coefficient and L the flame thickness. Unfortunately little data are available in the literature on K except for some common fuels.

Later on in this report, the steel temperature will be calculated using adiabatic surface temperatures (AST), calculated from measurements using plate thermometers. Detail on AST can be found in Appendix D.

To design fire safe constructions, predictions of thermal exposure can be estimated using the specifications in Eurocode 1, EN 1991-1-2 - Annex C – localized Fires. This method is described in Appendix C of this report and uses plume correlations to estimate gas temperatures in the plume from the burning rate. Since this work concentrates on the thermal exposure to the column we use the experimental values of fuel mass loss rate into the calculations. Thus, we know what is burning and the burning rate. However, there is still plenty of room for additional assumptions not covered by the Eurocode. Therefore, we have done two different fire designs, one resulting in a more severe thermal exposure than the other. The assumptions differ in the estimations of radiation from gases above the actual flame and the combustion efficiency. Details can be found in Appendix C.

1.2 Previous work

There are some experimental data from full scale fires available in the literature, such as the Murcia fire tests conducted in the large scale atrium with heptane pools of two diameters [4] with the main purpose to measure transient of gas and wall temperature as well as airflow at the inlets during fire in the large scale atrium. Some experimental data of the structural elements exposed to localized fires are available, such as unprotected ceiling slab [5, 6] and a two meter unprotected steel column [7]. Steel temperatures and heat flux were measured for further analysis. These studies focused mainly on correlations between experiment and simulations.

A limited series of tests with steel beams in a small room with dimensions according to the Room Corner Test ISO 9705) has previously been conducted at SP [8]. The beam was hanging 20 cm from the ceiling and a gas burner was placed in the corner and under the beam. The temperatures then measured by small thermocouples and plate thermometers (PT) were very different. That is because the PTs are much less sensitive to convection (they have a lower convective heat transfer coefficient) than the thermocouples. The PTs therefore adjust to temperatures very much dependent on the incident radiation to the

specimen surface. The study serves as an example of how to calculate the thermal exposure and the heat transfer to fire exposed surfaces using plate thermometer temperature measurements.

The work presented in this report summarizes full-scale experiments on a steel column exposed to various pool fires in a large room. The thermal exposure has been calculated according to the theories described in [9, 10]. Comparisons to Eurocode are presented. The effect of internal heat transfer within the column is discussed.

2 Experiments

The experiments were carried out in the large fire hall of SP, 20 m by 20 and 20 m high. A 6 m tall circular unprotected steel column with diameter 200 mm and a steel thickness of 10 mm was exposed to circular pool fires with various burning areas. The column was unloaded and its circular interior was left empty. The column was positioned centrally 20 cm above the fuel container in the middle of the fire hall under the main exhaust hood, see Figure 1. The lower and upper ends of the column were sealed. The column was fixed at the upper end hanging between two well insulated beams.



Figure 1 Experimental setup. Measurements were done at every metre along the column. Position 1 was in the left direction and position 2 was facing the mineral wool board.

Gas temperatures were recorded using thin thermocouples. Temperatures using plate thermometers (PTs) were also collected at every metre along the column as can be seen in figure 1. Four positions around the circumference were investigated. Position 1 was the most densely instrumented position (on the left hand side in figure 1). It was in the direction towards which the flames tilted during the experiments. Position 2 was facing an insulated wall for protecting measuring equipment (shown in the background of figure 1). Figure 2 shows the instrumentation on the column at 2 and 4 meters height. In position 1 and 3 standard plate thermometers were placed just outside the column surface. In position 2 and 4 embedded, extra insulated PTs, were included. In each position small thermocouples were also added for an estimation of gas temperatures. In addition to what is shown in figure 2, the steel temperature was measured above and under the PTs in position 1 and 3 (left and right in figure 2). A full description of the setup and the measurements can be found in Appendix A.

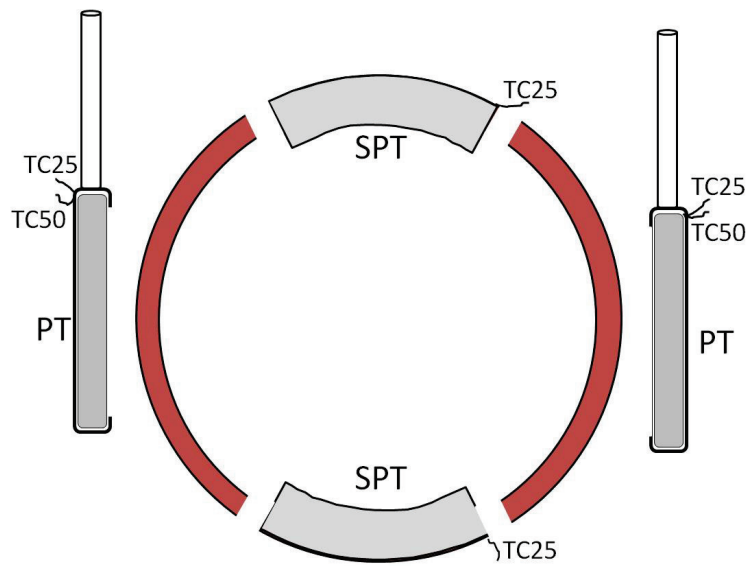


Figure 2 The instrumentation at 2 and 4 meters height.

The recorded fire exposures were from one diesel and one heptane fire of a circular pool with diameter and 1.1 m and a larger diesel fire from a pool of 1.9 m in diameter. Table 1 displays the calculated fuel characteristics.

Table 1. Fuel characteristics, mass loss rate, heat of combustion (ΔH_c), Heat release rate (HRR) and flame height.

Fuel	Mass loss rate (kg/s) [from experiment]	ΔH_c [9] (MJ/kg)	HRR [9] (MW) [based on mass loss rate]	Flame height (m) [from experiment]
Heptane, diameter 1.1 m	0.051	44.6	1.6	3.3
Diesel, diameter 1.1 m	0.032	39.7	1	2.6
Diesel, diameter 1.9 m	0.107	39.7	3.3	4.1

3 Results

3.1 Results from experiments

The mass loss rate, measured by the balance under the fuel pan, was constant with time during most of the burning period. The mass loss rates increased somewhat when the remaining fuel level was very low due to the heating of the pan itself. Linear best fits of the mass as a function of time gives mass loss rates of 0.051, 0.032 and 0.107 kg/s for heptane (1.1 m), diesel (1.1 m) and diesel (1.9 m), respectively.

All measurement results can be found in Appendix B or can be downloaded from the SP website [1] where a movie of the larger fire is also available. Even though no sideways draught could be noticed before the experiments the flames were clearly tilted towards position 1, see Appendix A for details. Figure 3 shows a series of pictures from the smaller diesel fire of diameter 1.1 m. Flames were flickering to a height between 2 and 3.5 m. Above 1 m the flame was most of the time tilted towards position 1 such that the column is visible from the opposite direction.



Figure 3. The flame from diesel $\varnothing = 1.1$ m. The flames are tilted towards position 1.

Increasing the pool diameter from 1.1 m to 1.9 m enlarged the size of the flames considerably. The height became then constantly over 4 m, sometimes reaching well over 5 m, see figure 4.

Temperatures of thermocouples and PTs along position 1 are presented in figure 5. It is evident that the small 0.25 mm thermocouples and the PTs in this case recorded essentially the same temperatures in this position. This was, however, not the case for all positions, e.g. at position 2 at 4 meters height, the PT temperature exceeded the gas temperature.

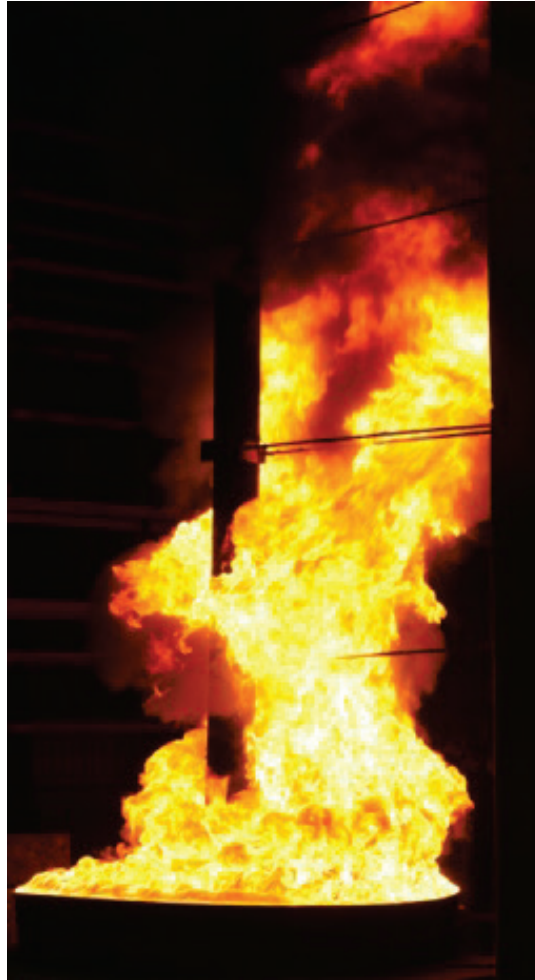


Figure 4. Photo of the large ($D=1.9$ m) diesel fire with over 4 m high flames tilting towards position 1.

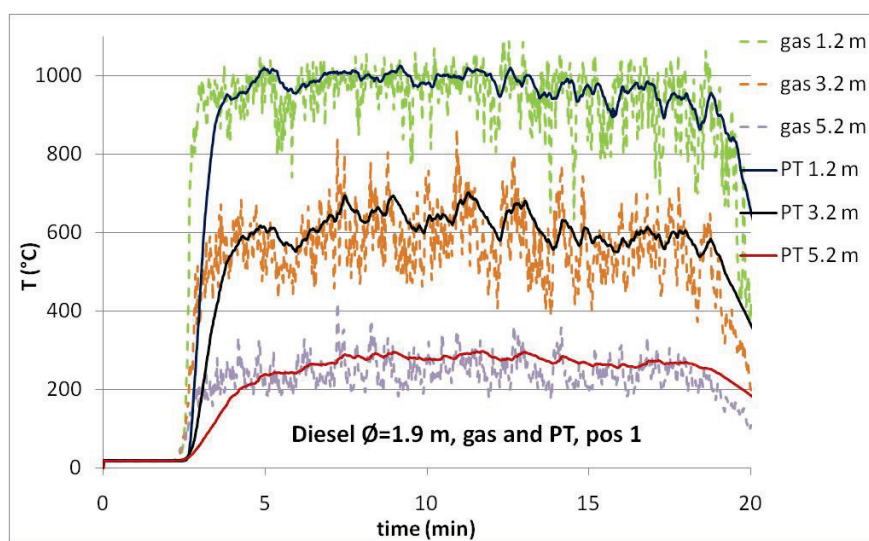


Figure 5. Measured gas and PT temperatures in position 1 for the larger diesel pool fire. The fuel was ignited at 2 minutes.

As the flame tilted towards position 1, the thermal transfer was asymmetric which was clearly indicated by the PT measurements. Figure 6 shows PT temperatures around the column at 2 meters height and displays a difference between positions 1 and 2, and positions 3 and 4 of more than 200 °C. The corresponding data at 4 meters height is shown in figure 7, indicating the same asymmetry. Naturally, the asymmetric thermal exposure of the column had consequences on the steel temperatures. From the movie [1] one can for example observe the curvature of the column due to uneven thermal expansion.

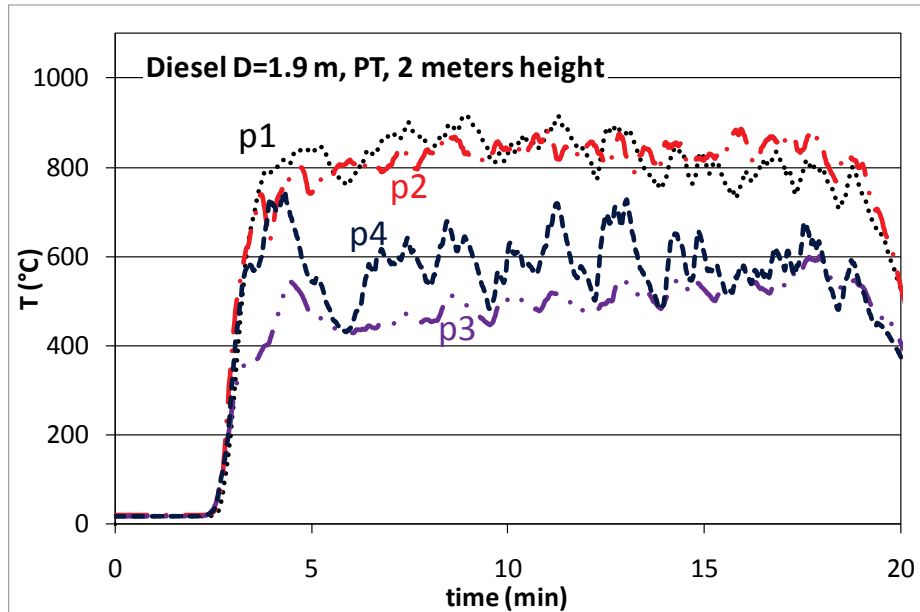


Figure 6. PT temperatures at 2 m height of the column. The four curves represent the different positions around the circumference of the column.

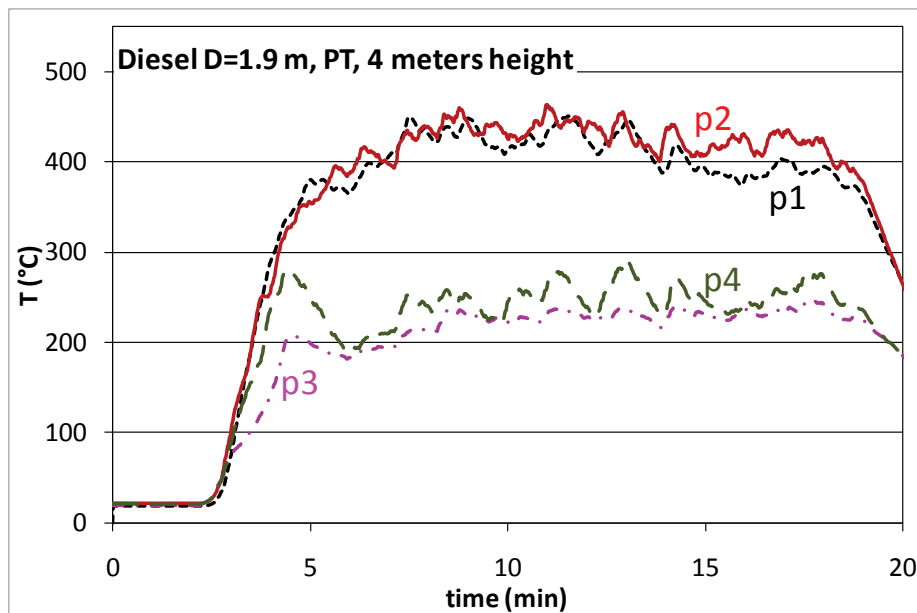


Figure 7. PT temperatures at 4 meters height of the column. The four curves represent the different positions around the circumference of the column.

The recorded steel temperatures for the diesel fire with $\text{Ø} = 1.9 \text{ m}$ are shown in figure 8. The corresponding data for the $\text{Ø} = 1.1 \text{ m}$ diesel fire and the heptane fires are shown in figure 9 and 10, respectively. The hottest region was close to the fire source where the steel reaches almost 800 °C at 1 m height after about 15 minutes of fire exposure. The temperature decreased with height. At 2 m the difference between position 1 and 3 (opposite each other) is very big. After 8 minutes of fire the difference was as much as 250 °C . By analysing the shapes of the steel temperature curves, it is clear that heat was transferred to the colder region of the column which evens out the temperature differences between position 3 and 1. Given a thermal diffusivity of approximately $10^{-5} \text{ m}^2/\text{s}$ (which yields a characteristic diffusion time of two hours over half the circumference), heat conduction along the periphery of the column could only account for a minor part of this heat transfer. The dominating mechanism must have been radiative exchange between the inside surfaces of the column.

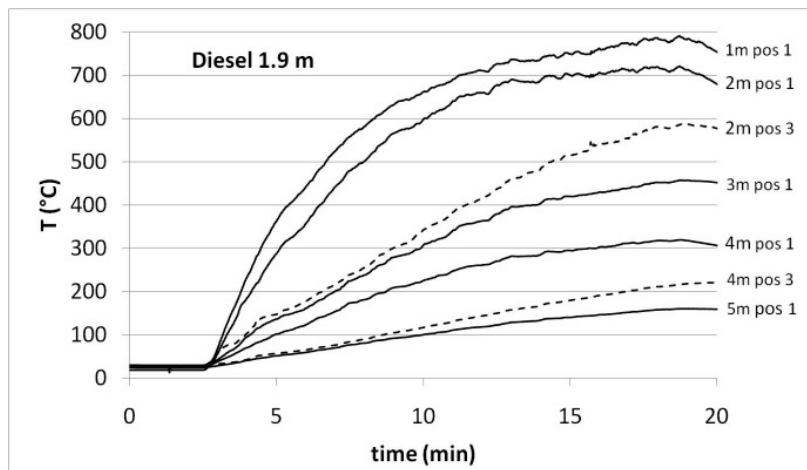


Figure 8. Measured steel temperatures for the larger diesel fire ($\text{Ø} = 1.9 \text{ m}$). Solid and dashed lines represent position 1 and 3, respectively.

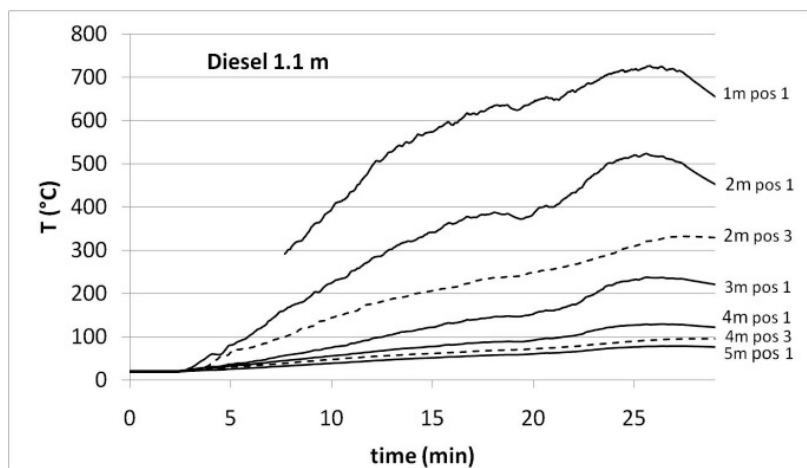


Figure 9. Measured steel temperatures for the smaller diesel fire ($\text{Ø} = 1.1 \text{ m}$). Solid and dashed lines represent position 1 and 3, respectively.

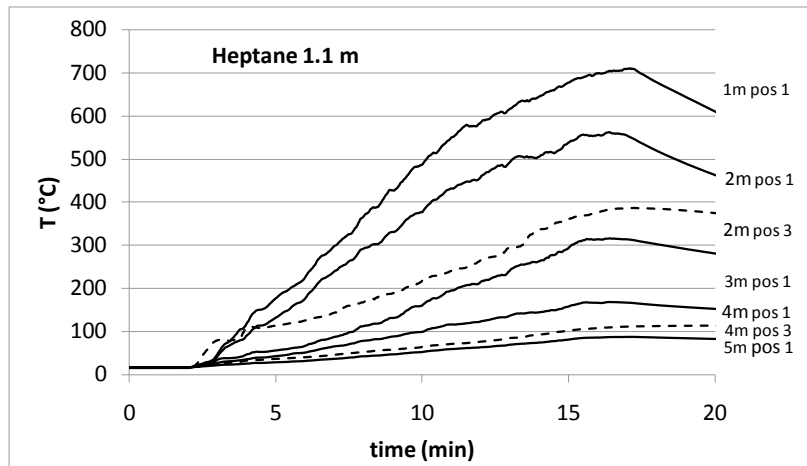


Figure 10. Measured steel temperatures for the heptane fire ($\varnothing = 1.1$ m). Solid and dashed lines represent position 1 and 3, respectively.

3.2 Comparison with Eurocode calculations

The thermal action was also calculated from the specifications in Eurocode 1 EN 1991-1-2 (Equations (C1-C7)). For these calculations we use the mass loss rate from experiments such that we have the correct input on what is burning and how fast. The exposure is calculated through the gas temperatures in the plume, which in turn are specified in the Eurocode according to the Heskestad plume correlation [2]. However, this correlation is not valid for temperatures exceeding 900 °C. In situations where the correlation exceeded this limit (close to the fuel surface) the temperature was fixed to 900 °C in order not to overestimate the temperature of the gas.

Nevertheless, there are still unknown parameters in the equations given by the Eurocode, where default values are given if no other information is available. Two such parameters are the combustion efficiency and the radiation (emissivity) from the gas plume above the flames. For this study we perform two sets of calculations including extreme values of these parameters such that we yield an upper and a lower bound on the thermal exposure, calculated according to the specifications in Eurocode 1. Details on how these calculations were performed are specified in Appendix C. Other versions of these calculations have been presented in other publications [11, 12].

Once again, the asymmetry of the flame induced a large temperature differences around the circumference of the column at any height. However, it is worth noting that at each height and for each fuel the lowest possible temperature estimate using Eurocode (i.e. the low impact assumptions discussed above) exceeds the highest measured value with only one exception. This exception occurred close to the large diesel fuel surface where 950 °C are measured. The Eurocode does not describe correlations for temperatures above 900 °C.

Table 2. Gas temperatures after 10 minutes.

Fuel and pan diameter	Height above fuel surface (m)	T _{gas} , (°C)*	T _{gas} Eurocode (°C)	T _{steel} , (°C)	T _{steel} Eurocode (°C)
Heptane, diameter 1.1 m	1.2	900	900	584	747
	2.2	300-650	900	265-457	747
	3.2	500	661-883	214	514-706
	4.2	150-280	353-442	76-122	204-280
	5.2	180	260-325	63	97-183
Diesel, diameter 1.1 m	1.2	800	900	495	747
	2.2	250-500	720-900	175-281	583-747
	3.2	250	363-455	96	212-292
	4.2	110-150	212-263	54-65	82-141
	5.2	120	162-200	44	66-104
Diesel, diameter 1.9 m	1.2	950	900	711	747
	2.2	480-800	900	415-660	747
	3.2	640	825-900	363	699-747
	4.2	220-400	464-583	144-261	301-426
	5.2	250	347-435	118	200-248

*Measured gas temperatures from position 1 when only one value is given. At heights where temperatures were probed around the column values are given in intervals.

The differences between the fire temperatures from experiment and Eurocode calculations have also an impact on the resulting steel temperatures, see table 2. The Eurocode temperature estimations were always higher than the measured values, even when comparing the estimations calculated using the lowest possible heat transfer to the maximum experimental values (position 1). Figure 11 shows the comparison of the measured steel temperature and calculated according to the EN 1991-1-2 [13].

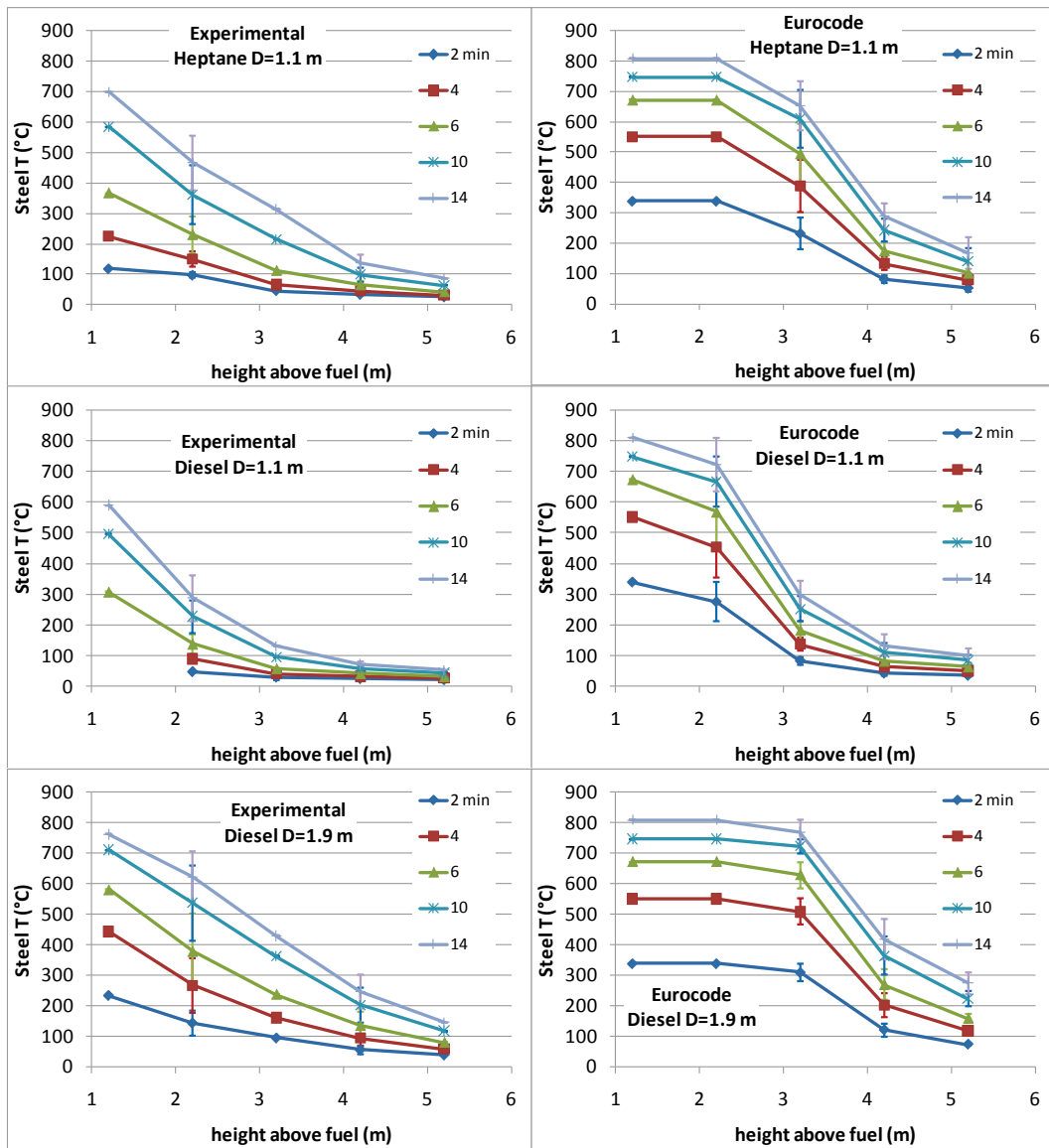


Figure 11. Measured steel temperatures (left), calculated steel temperatures according to the EN 1991-1-2 (right). The error bars in the experimental data represent the highest and lowest measured values (usually position 1 and 3). The error bars in the calculated data represent the two different interpretations of the Eurocode.

3.3 FEM calculations

Using the PT and gas temperature readout, the AST can be calculated according to the method described in Appendix D and specified in [14]. These values are thereafter used as input to finite element simulations for the $\varnothing = 1.9$ m diesel fire at 2 and 4 meters along the column. AST is used as the effective fire temperature from which the total heat flux to the column is calculated according to

$$\dot{q}''_{tot} = \epsilon_s \sigma (T_{AST}^4 - T_s^4) + h_c (T_{AST} - T_s) \quad (8)$$

In this case the AST is very close to the PT temperatures for those positions. The thin thermocouples and PT show almost the same temperature.

Since we have measurements at all 4 positions at heights 2 and 4 meters we can calculate AST at each position and run a FEM model in TASEF to calculate the corresponding temperatures. The emissivity of the steel is set to 0.8 and the convective heat transfer coefficient to 25 W/m²K. The column is approximated to a quadratic section of the same thickness. The size of the sides is such that the mass of the real and the model columns are the same. The cell distribution is shown in Figure 12.

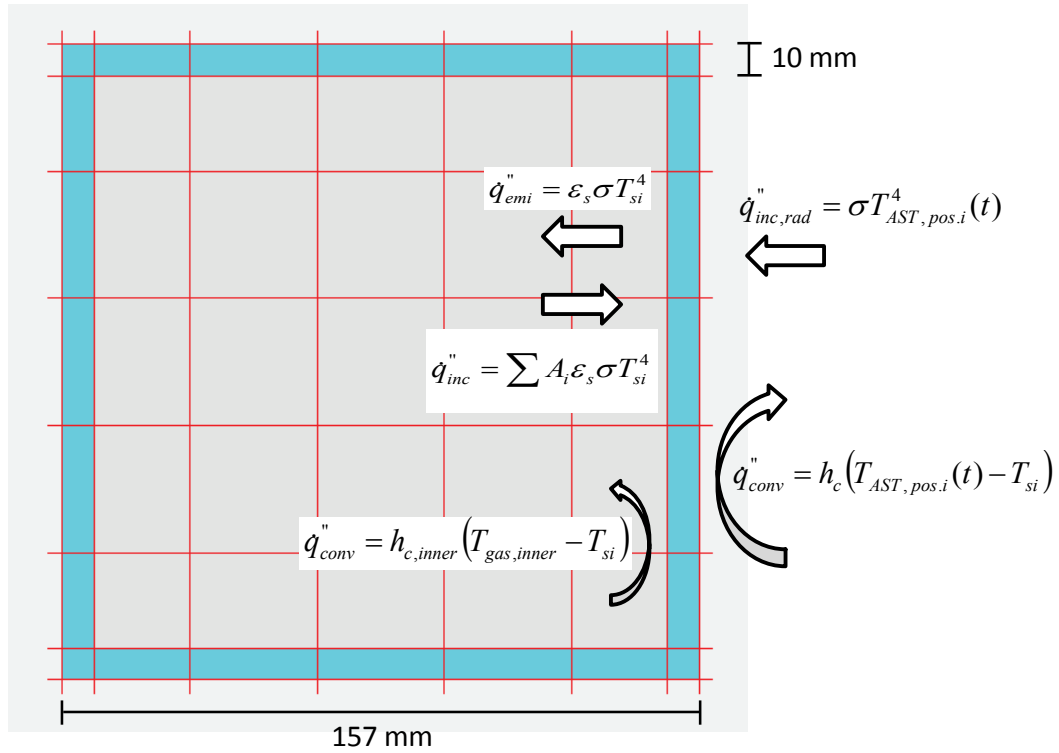


Figure 12. The cell distribution for the 2-D FEM analysis. The boundary conditions for one side are shown. On each side the AST calculated from each PT is used.

In order to describe also the later stage of the fire where considerable heat is transferred within the column from the hotter to the colder side we allowed for radiative heat transfer between the inner surfaces. A small convective contribution is also included with a heat

transfer coefficient of $1 \text{ W/m}^2\text{K}$. Comparison with experiment where this inner heat transfer is not taken into account is shown in Appendix E.

Comparisons between FEM calculations and the experiments are shown in figure 13. The measured and simulated values match very well despite the unstable and inhomogeneous nature of the flame. This suggests that PT measurements yield very valuable data for expressing the intensity of thermal exposure as was earlier shown for a beam [8].

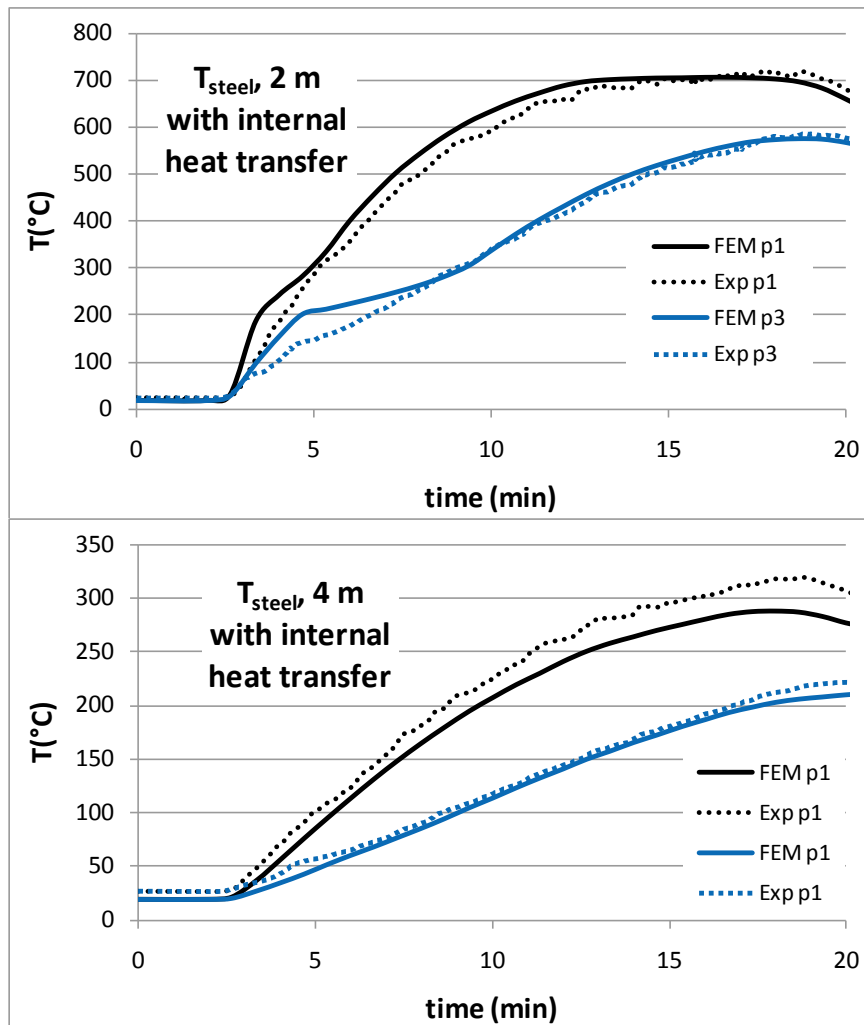


Figure 13. Steel temperatures of the column in position 1 and 3 as measured in the 1.9 m diesel fire (dotted lines) and as obtained from the finite element simulation using Eq. (8) as boundary condition (solid lines). Upper: 2 m along the column. Lower: 4 m along the column.

4 Summary and conclusions

This study gives unique reference data on steel, gas and PT temperatures for a full scale column exposed to localized fires. The fires studied were two different sized diesel pool fires ($\varnothing = 1.1$ and 1.9 m) and one heptane pool fire ($\varnothing = 1.1$ m). The data is available for downloading on the SP website [1].

The results show that for such large engulfing flames with high gas velocities as the ones studied here the temperatures of the PTs and thin thermocouples are more or less the same. This could be the consequence of both thermally thick flames (gas- and radiation temperatures are the same) and high gas velocities.

Even though no significant draught was observed prior to the tests, the flames were tilted in one direction (towards position 1). This yielded an asymmetric thermal exposure with temperature differences of up to 250 °C between different positions around the column periphery at the same level. This asymmetric exposure induced a curvature in the longitudinal direction due to the uneven thermal expansion over the cross section. This curvature may induce secondary bending moments in an axially loaded column. It is noted, however, that in the case of the circular column section internal heat transfer evens out the temperatures.

The method described in Eurocode 1 for calculating plume temperatures gives conservative results for gas and steel temperatures when compared with the results of the experiment, as expected.

However, comparing measured and predicted steel temperatures using the Eurocode formulation is not straightforward. In this study, both the response of the whole column section and that of 2-D cross sections at 2 and 4 meters along the column were evaluated. Using the lumped heat capacity approach for the entire section the effect of non-uniform heating arising from the plumes eccentricity is not considered. When evaluating the 2-D cross sections of steel exposed to the measured gas temperatures the calculated temperature on the less exposed side (position 3) is lower than the measured temperature. Likewise, the calculated temperature at the more exposed side (position 1) is higher than the experimental values. This is attributed to radiative exchange across the gap in the column: heat will be lost through radiation from position 1 and gained at position 3. More investigations concerning the Eurocode assumptions for lumped capacitance of steel sections are called for.

This report also shows that the PT readout, transformed to AST can be used with good success to calculate the thermal development of the steel structure. In the case studied here it is also important to employ a thermal model which considers the internal cross section heat exchange by radiation and convection.

5 References

- [1] http://www.sp.se/en/index/services/localized_fire/Sidor/default.aspx
- [2] Heskestad, G., Fire Plumes, Flame height and Air entrainment, SFPE Handbook of Fire Protection Engineering, 3rd edition, National Fire Protection Association, Quincy, MA 2002.
- [3] McCaffrey, B.J., Purely Buoyant Diffusion Flames: Some Experimental Results, Fire Safety Journal, vol 3, pp 107-121, 1980.
- [4] Guttierrez-Montes C., Sanmiguel-Rojas E., Vieda A., Rein G., Experimental data and numerical modeling of 1.3 and 2.3 MW fires in a 20 m cubic atrium, Building and Environment, Vol: 44, i: 9, pp 1827-1839.
- [5] Hasemi Y., Yokobayashi Y., Wakamatsu T., Pchelintsev A.V., Modeling of the heat mechanism and thermal response of structural components exposed to localized fires: A new application of diffusion flame modeling to fire safety engineering, 13th meeting of the UJNR panel of fire research and safety, Vol 1, March, 1996.
- [6] Wakamatsu T., Hasemi Y., Pchelintsev A.V., Heating mechanism of building components exposed to a localized fire. CFD prediction to a localized fire, Fire science & technology, Vol 20, No1, 2000.
- [7] Li G.-Q., Zhang C., Thermal response of steel columns exposed to localized fires – numerical solutions and comparison with experimental results, Journal of Structural fire engineering, Vol 2, No 4, 2011.
- [8] Jansson R., Wickström U., Tuovinen H., Validation fire tests on using the adiabatic surface temperature for predicting heat transfer, SP Report 2009:19.
- [9] Babrauskas V., Heat release rate, SFPE Handbook of Fire Protection Engineering, 3rd edition, National Fire Protection Association, Quincy, MA 2002.
- [10] Karlsson B., Quintiere J.G., Enclosure fire dynamics, CRC Press, Boca Raton, FL, 2000.
- [11] Byström A., Sjöström J., Wickström U. and Veljkovic M., Large scale test to explore thermal exposure of column exposed to localized fire, proceedings of Structures In Fire, Zürich, 2012.
- [12] Byström A., Sjöström J., Wickström U. and Veljkovic M., A steel column exposed to localized fire, Nordic Steel, Oslo 2012.
- [13] Franssen J.M. and Real P.V., Fire Design of Steel Structures, 1st edition, Ernst & Sohn, Berlin, 2010, 17-45.
- [14] Byström A., Cheng X., Wickström U., Veljkovic M., Measurement and calculation of adiabatic surface temperature in a full-scale compartment fire experiment, Journal of Fire Sciences, Vol. 31, p. 35, 2013.
- [15] Häggkvist A., Sjöström J., Wickström U. Using plate thermometer measurements to calculate incident heat radiation, Journal of Fire Sciences, Vol 31, pp 166-177, 2013.

Appendix A – Instrumentation

Column and setup

The column is a six meter long steel column, denoted S355J2H. Its outer diameter is 203 mm and the thickness of the steel is 10 mm. The bottom of the column is plugged with a steel disc and the top was plugged with mineral wool (5 cm thick). The column was hanging from an insulated steel beam eight meters above the floor. The lower end of the column was 20 cm from the pool surface at start of each experiment.

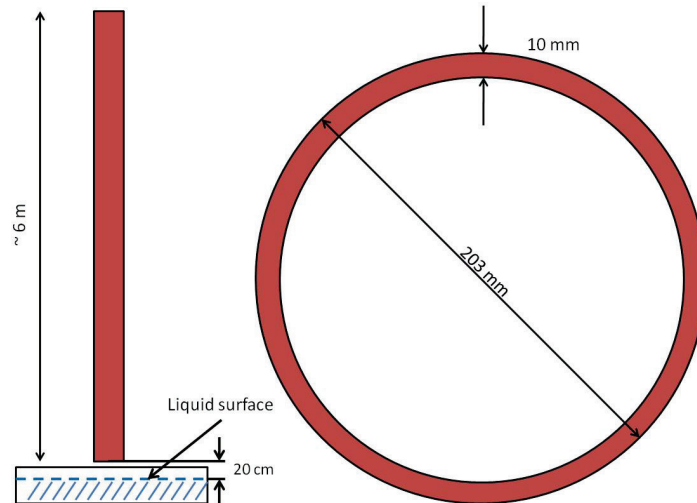


Figure A1 The experimental setup showing the dimension of the column and the placement relative the pool.

At a distance of 2.5 meters from the column a mineral wool insulation board was placed to protect a column used for attaching plate thermometers and collecting thermocouples from the fire exposed column.

Three tests were conducted with the following fuels and circular pools:

1. Diesel, pool \varnothing 1.1 m (0.95 m²).
2. Heptane, pool \varnothing 1.1 m (0.95 m²).
3. Diesel, pool \varnothing 1.9 m (2.83 m²).

The mass of the fuel was continuously monitored using a balance under the pool.



Figure A2 Picture of the experimental setup. Position 1 is in the right direction and position 2 is facing the mineral wool board.

Instrumentation

Along the column different types of thermocouples were installed at one meter distance starting from 1 meter from the lower column end. The different types of thermocouples are listed below.

TC25. Welded thermocouples, 0.25 mm in diameter.

TC50. Shielded thermocouples, 0.5 mm in diameter with the ability to resist high temperatures.

PT. Standard plate thermometers as defined in the international fire resistance furnace test standard ISO 834.

SPT. Specially designed plate thermometers with a 100 cm² square surface of 0.4 mm thick Inconel600 alloy (compared to 0.7 for standard PT). The SPTs are insulated with 20 mm Superwool ceramic insulation from Isover and is attached to a steel plate at the back with four “arms” according to figure A3. The SPTs were all pre-treated in a furnace

during two hours at 1000 °C to burn out any residuals contributing to exothermic reactions during heat-up and to increase the surface emissivity of the Inconel surface. The SPTs used on the column were curved and embedded into the column at certain voids with a small air gap of a few mm between SPT and steel, see figure A4. SPTs with a flat surface were also designed to be used



Figure A3 The specially designed plate thermometers that were embedded in the steel column flush with the surface.

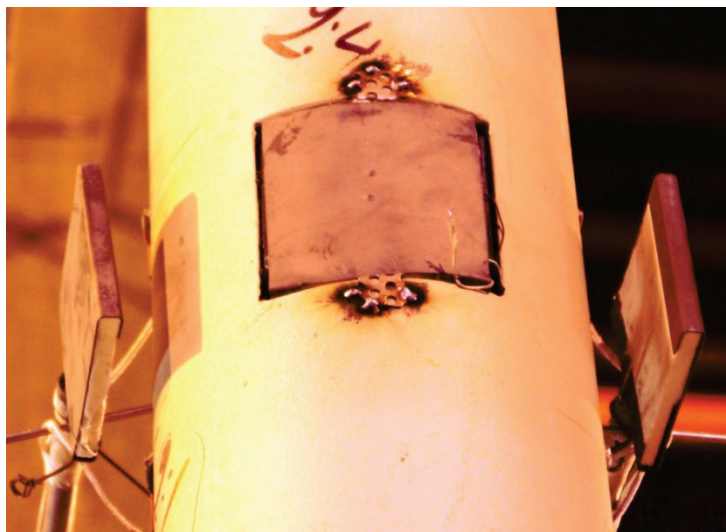


Figure A4 Picture showing embedded plate thermometer in position 2 and standard plate thermometers in positions 1 and 3.

QT. Thermocouples (Cefir ®) with quick-tip placed into drilled holes and fixed by a punch mark in the nearby metal, see figure A5.



Figure A5 Quick tip with Cefir cable fixed in the steel structure.

In addition we measured the heat transfer to a cooled surface facing the fire using a Schmidt–Boelter heat flux meter (HFM).

The column was instrumented at five different heights according to figure A6.

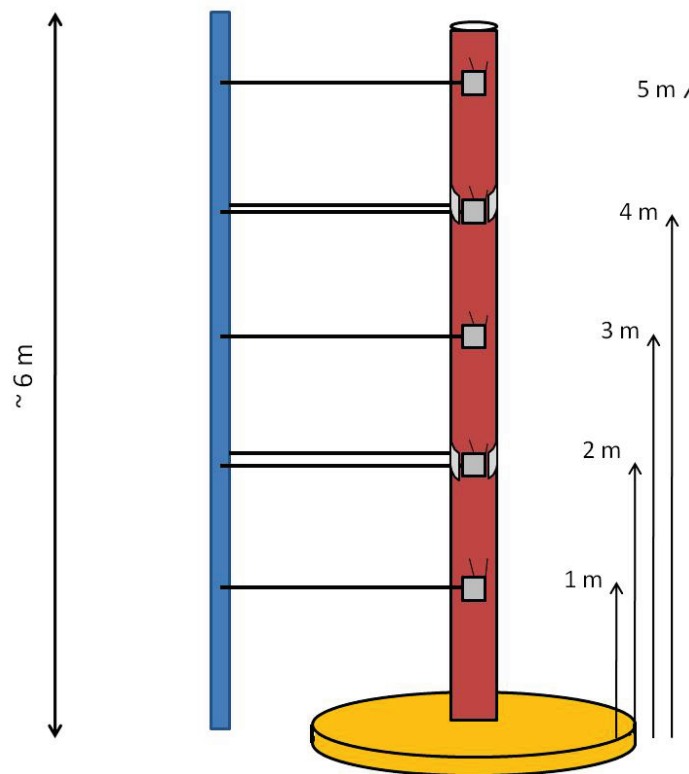


Figure A6 Sketch of the instrumentation.

Four directions from the centre of the column is defined and hereafter referred to as position 1 to 4. Position 1 is most dense in instrumentation and represents the right

direction in figure A2. Position 2 is in the direction 90° clockwise from position 1, thus facing the insulation board as shown in figure A2. Position 3 and 4 are each 90° rotated from the previous, see figure A7. All instruments at each height are described below.

1 meter. PT, TC25, TC50 and steel in position 1, see figure A7.

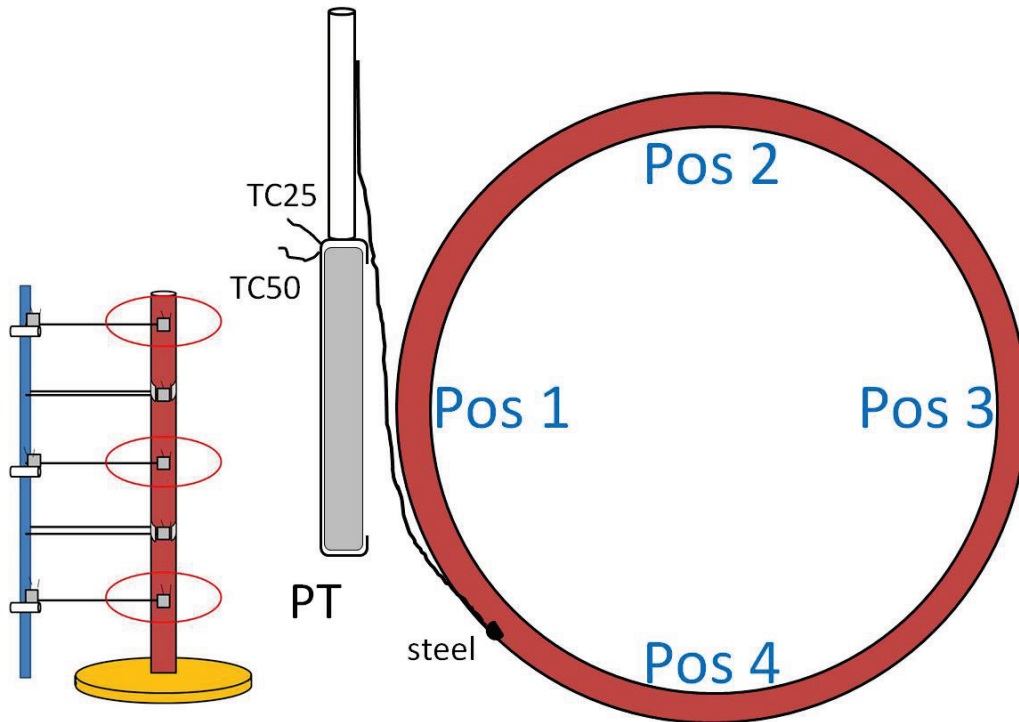


Figure A7 The instrumentation at 1, 3 and 5 meters height.

2 meters.

Pos 1: PT, TC25, TC50

Pos 2: SPT and TC25

Pos 3: PT, TC25, TC50

Pos 4: SPT and TC25

In addition QT are mounted on position 1 and 2, 5 mm over and under the edge of the PT, see figure A9.

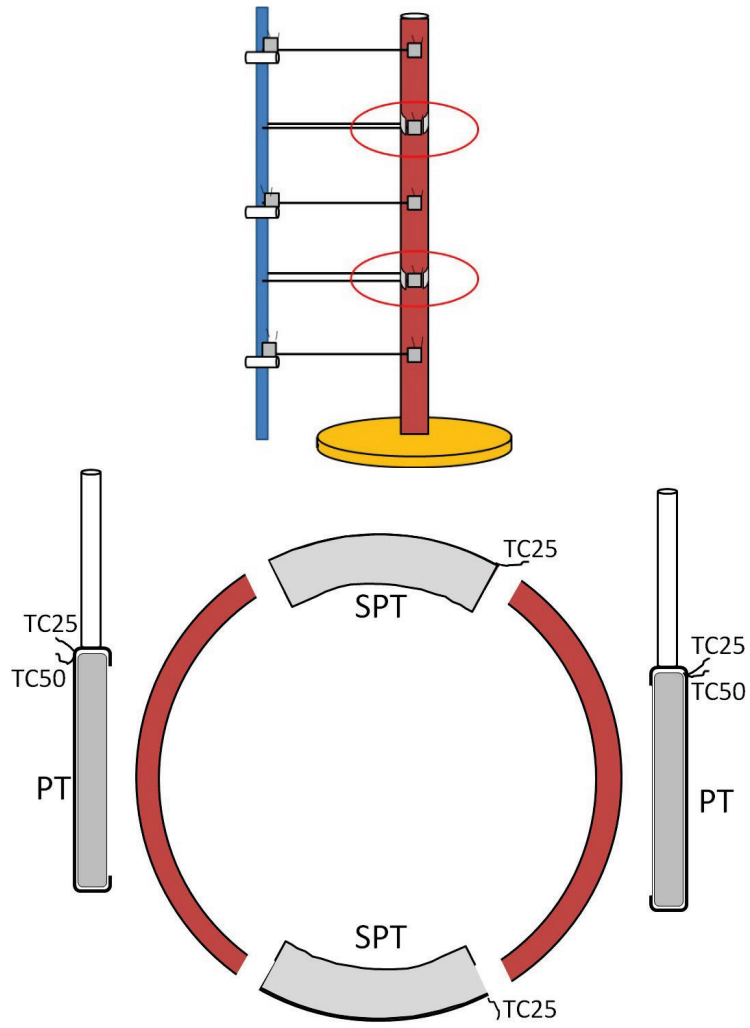


Figure A8 The instrumentation at 2 and 4 meters height. At 4 meters there is no TC50 at position 3.

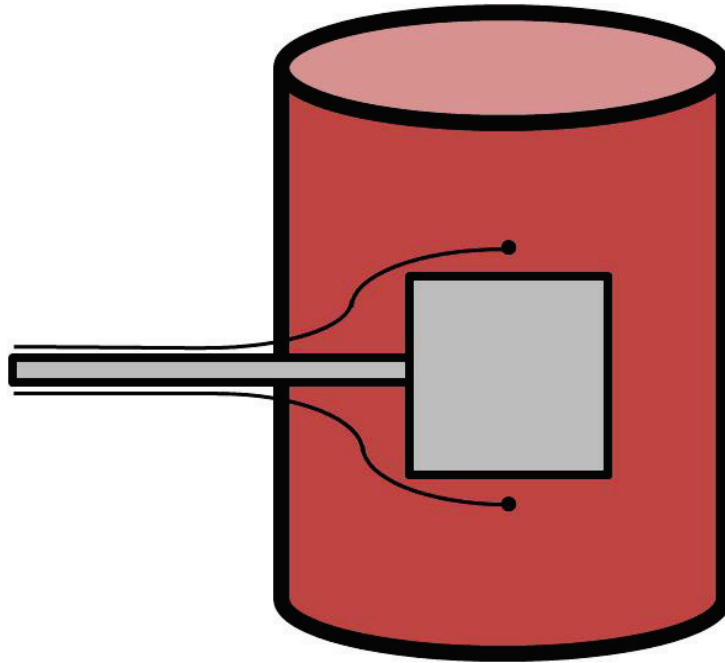


Figure A9 The position of the steel QTs at 2 and 4 meters height. The figure is facing position 1 or 3.

3 meters. Same as 1 meter: PT, TC25, TC50 and steel in position 1.

4 meters. Same as 2 meters but no TC50 in pos. 3.

5 meters. Same as 1 meter: PT, TC25, TC50 and steel in position 1.

On the external mineral wool board we have measuring positions at 1, 3 and 5 meters. All of them face the column position 2. Instruments include for all heights: PT, flat SPT, TC25 and HFM.

Appendix B – Results

Diesel fire Ø=1.9 m

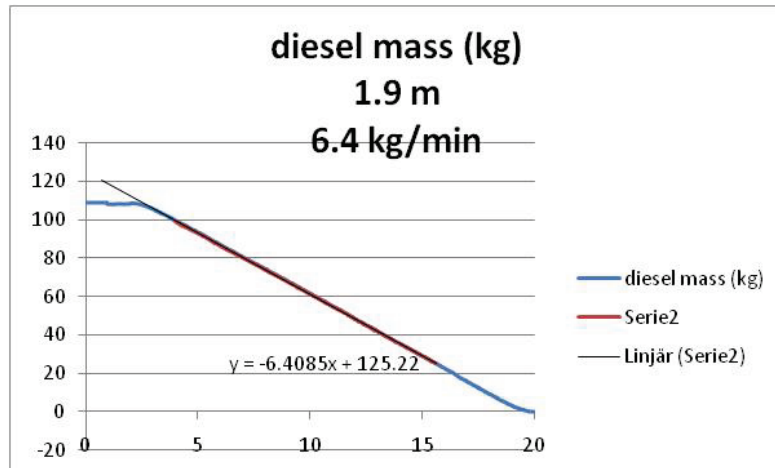


Figure B1 Mass loss of the fuel. X-axis is time un unit (min) and y-axis is mass of the fuel in (kg).

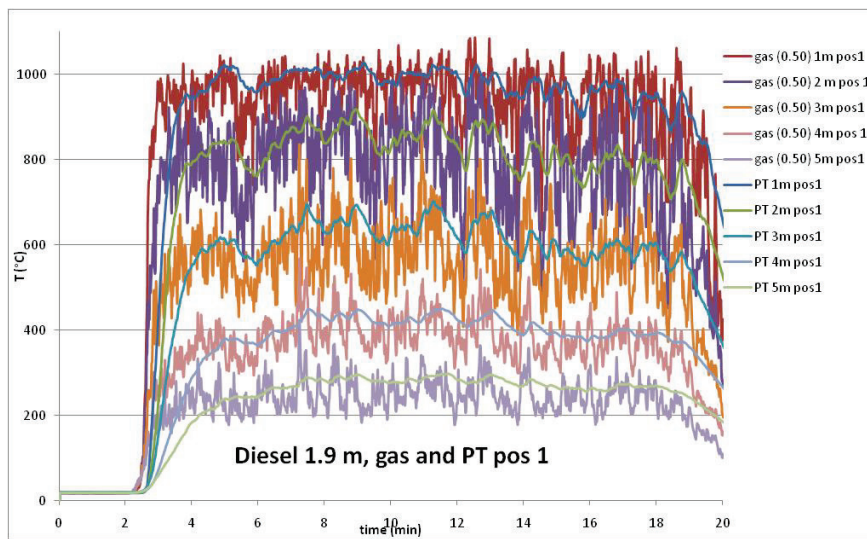


Figure B2 Gas and PT temperatures in position 1.

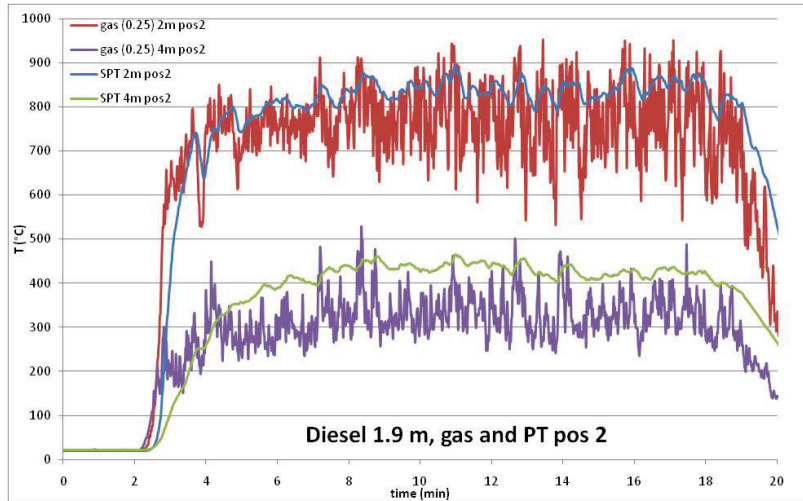


Figure B3 Gas and PT temperatures in position 2.

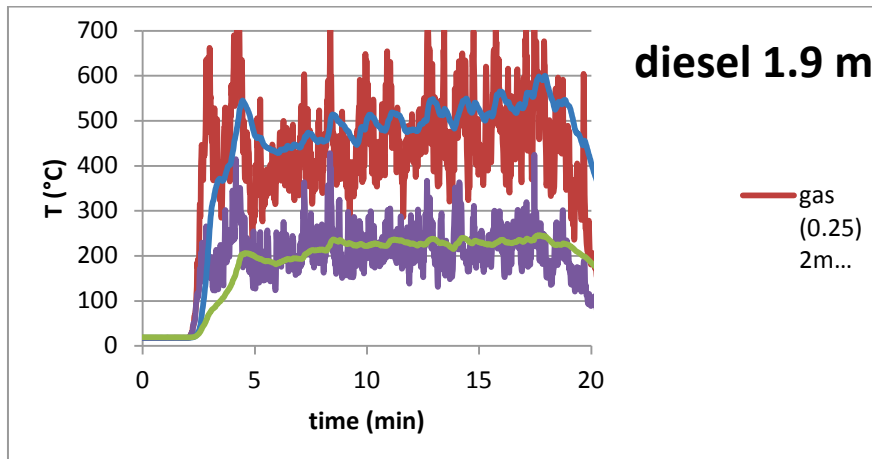


Figure B4 Gas and PT temperatures in position 3.

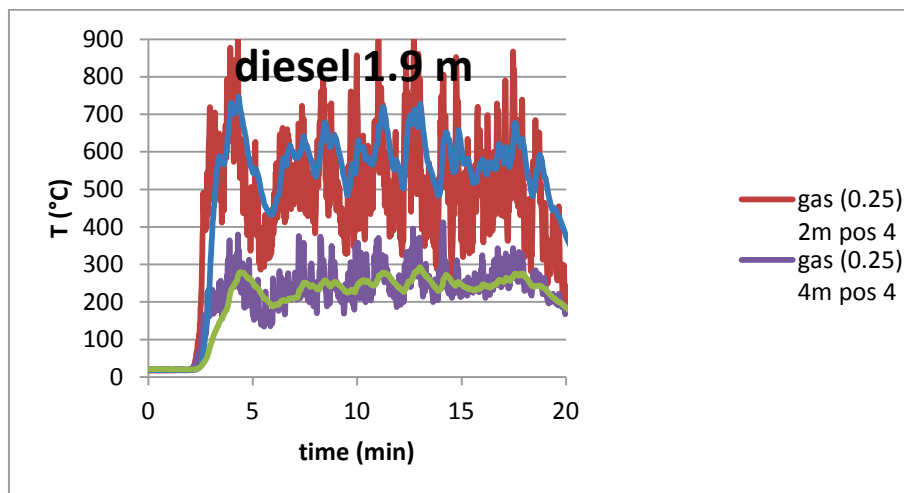


Figure B5 Gas and PT temperatures in position 4.

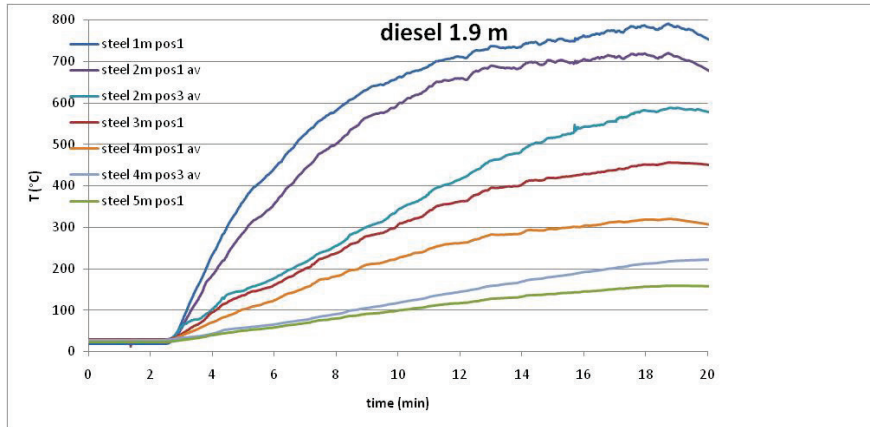


Figure B6 Steel temperatures.

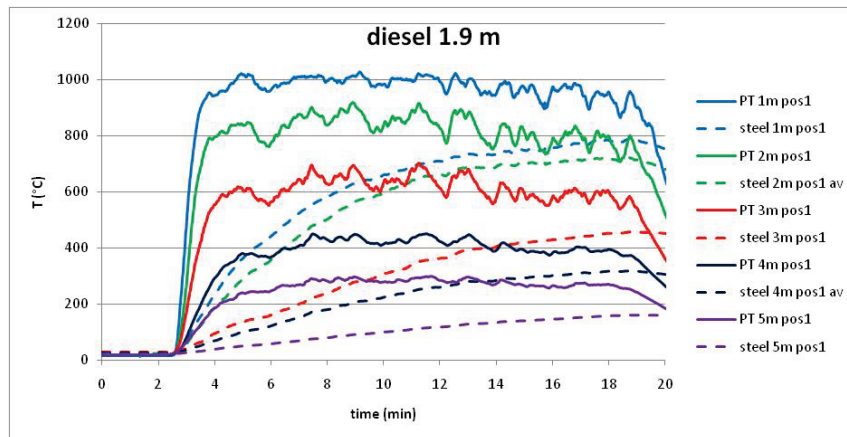


Figure B7 Comparison of PT and steel temperatures.

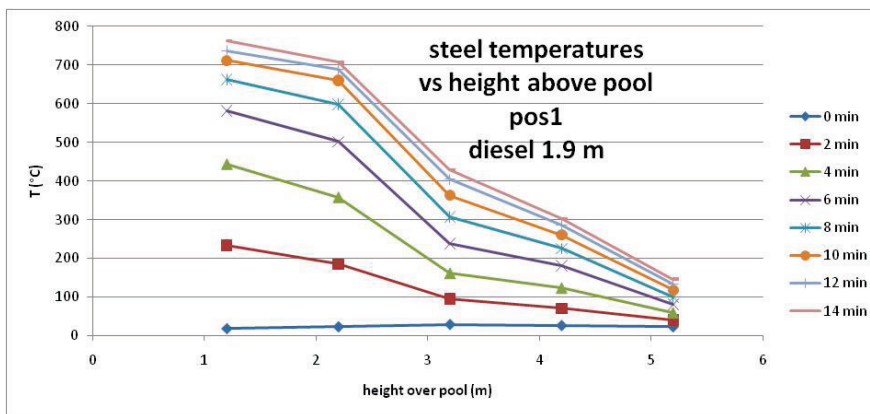


Figure B8 Steel temperatures along the column height for different times.

Heptane fire $\varnothing=1.1$ m

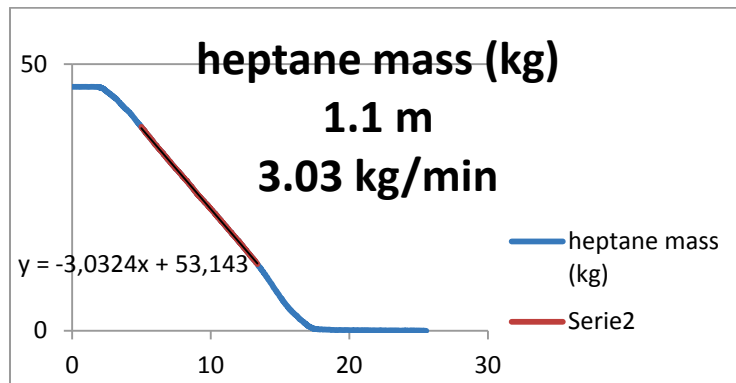


Figure B9 Mass loss of the fuel. X-axis is time un unit (min) and y-axis is mass of the fuel in (kg).

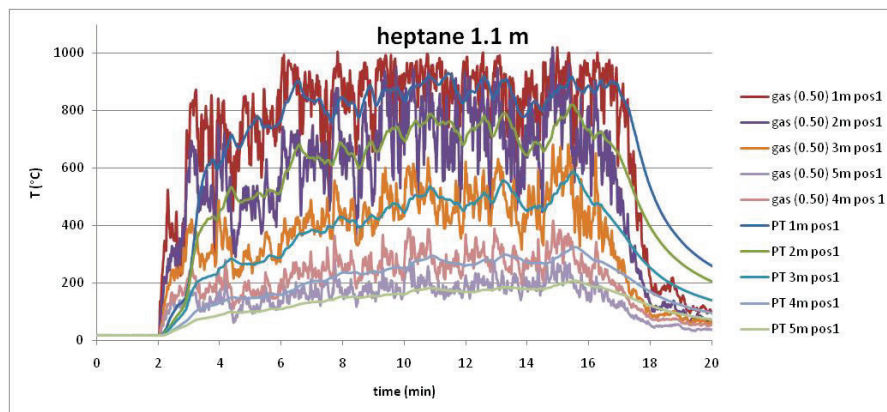


Figure B10 Gas and PT temperatures in position 1.

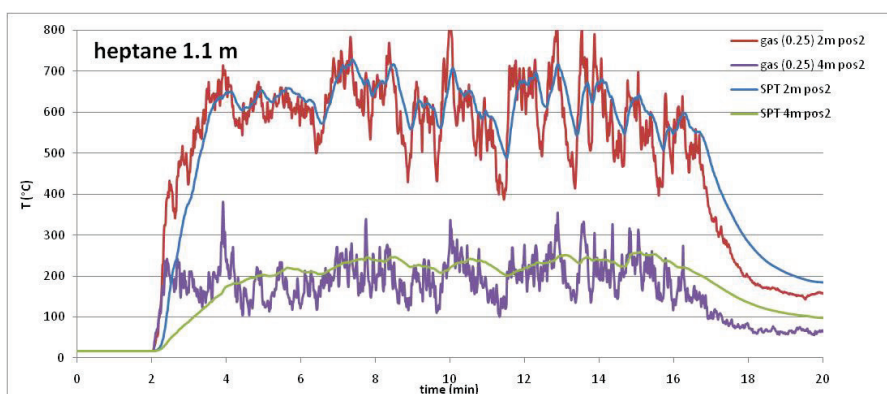


Figure B11 Gas and PT temperatures in position 2.

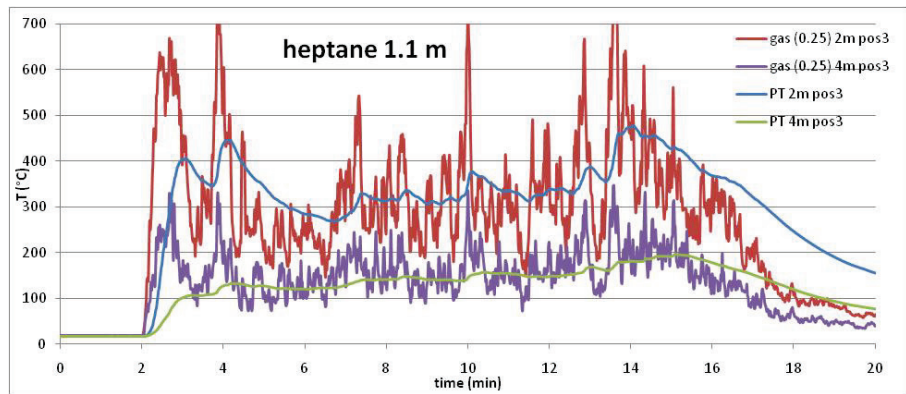


Figure B12 Gas and PT temperatures in position 3.

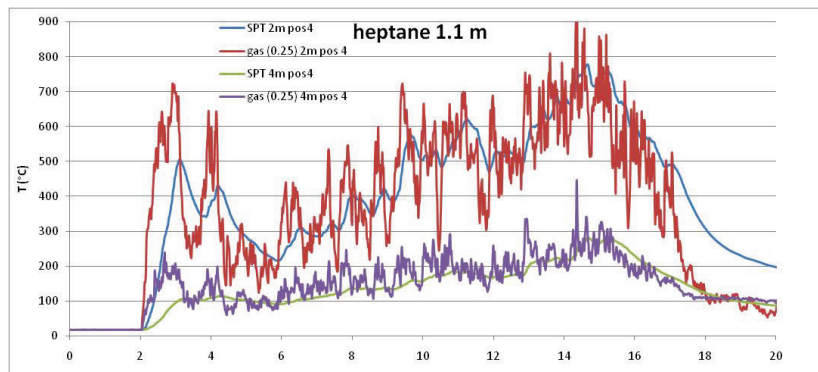


Figure B13 Gas and PT temperatures in position 4.

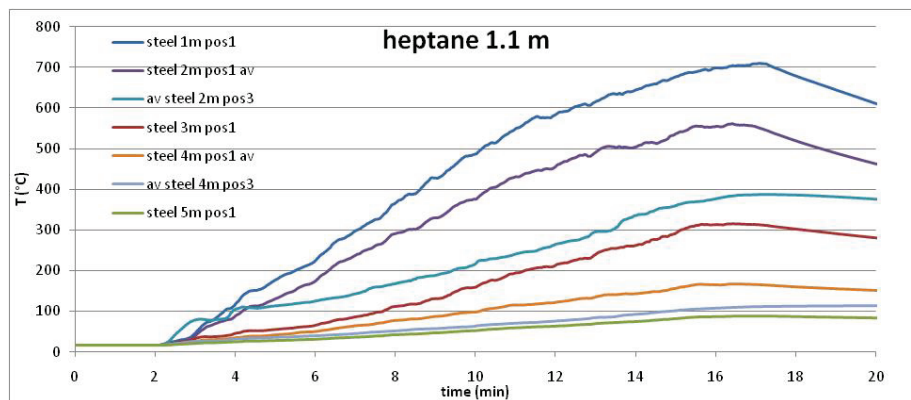


Figure B14 Steel temperatures.

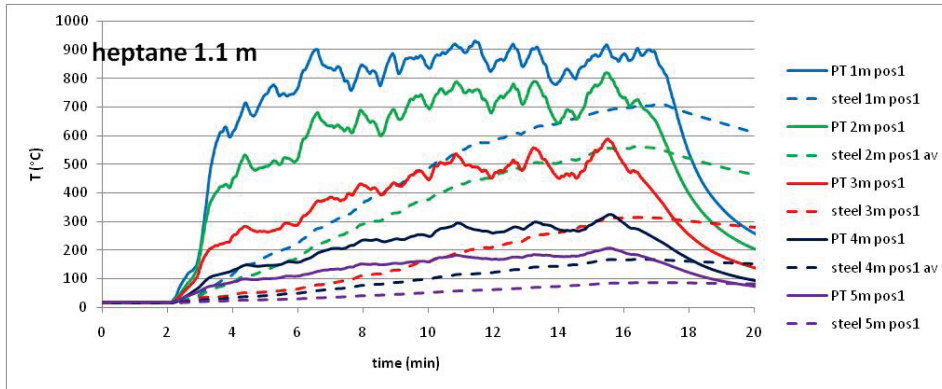


Figure B15 Comparison of PT and steel temperatures.

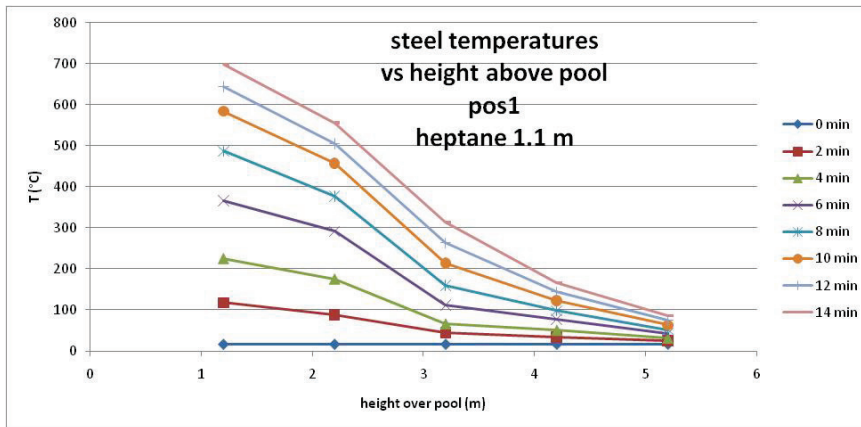


Figure B16 Steel temperatures along the column height for different times.

Diesel fire Ø=1.1 m

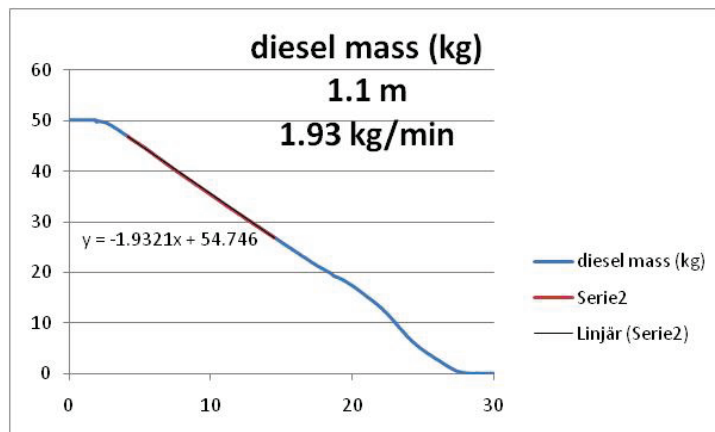


Figure B17 Mass loss of the fuel. X-axis is time un unit (min) and y-axis is mass of the fuel in (kg).

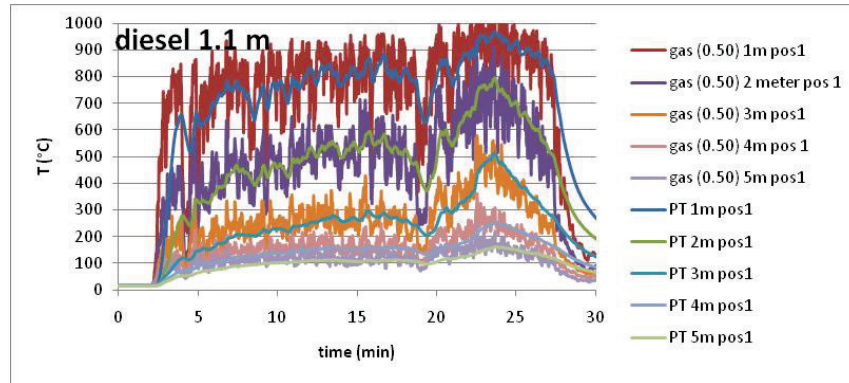


Figure B18 Gas and PT temperatures in position 1.

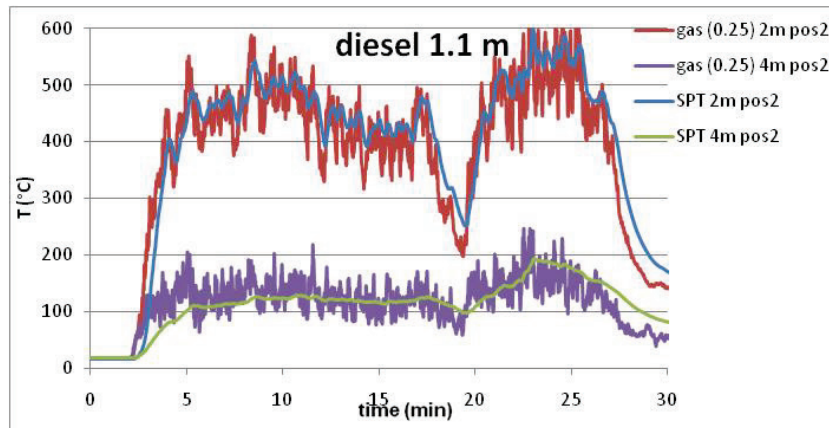


Figure B19 Gas and PT temperatures in position 2.

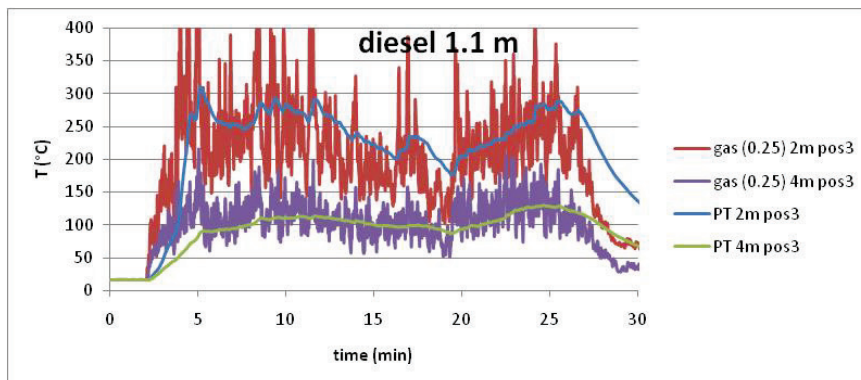


Figure B20 Gas and PT temperatures in position 3.

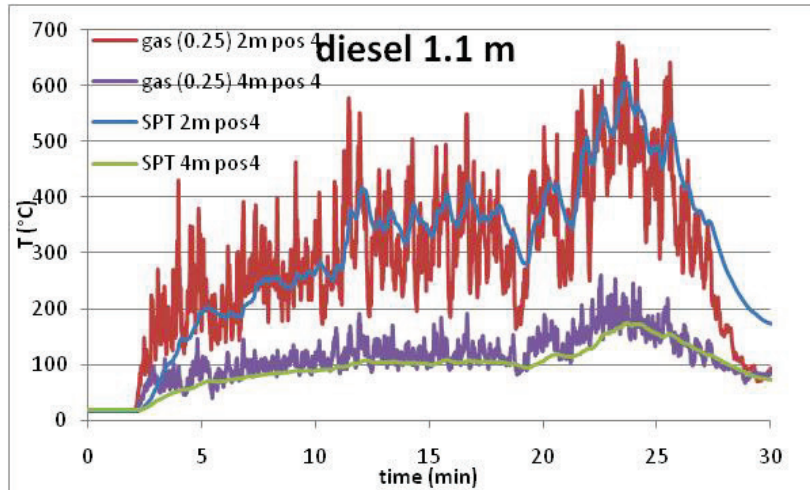


Figure B21 Gas and PT temperatures in position 4.

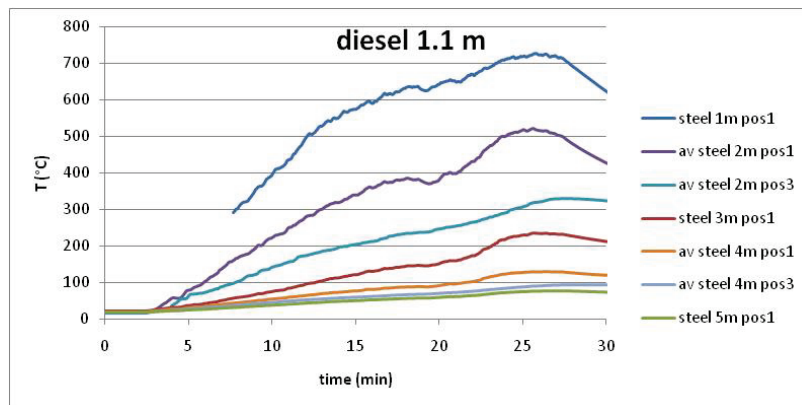


Figure B22 Steel temperatures.

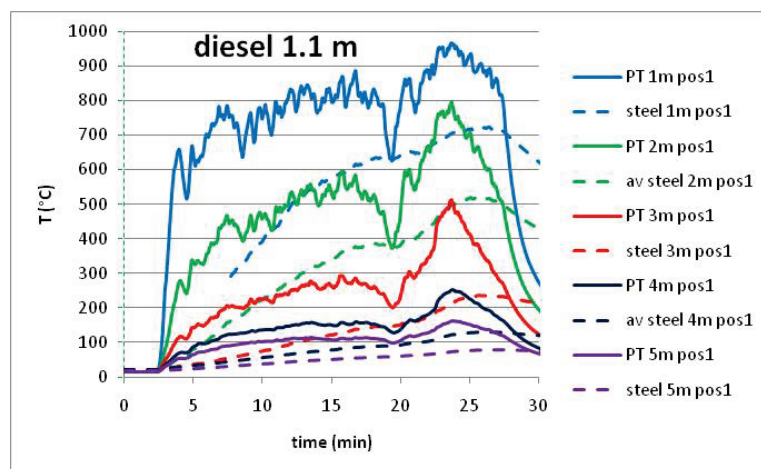


Figure B23 Comparison of PT and steel temperatures.

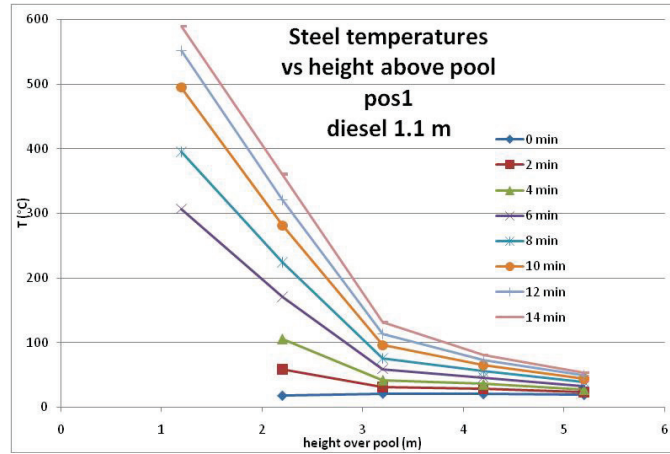


Figure B24 Steel temperatures along the column height for different times.

Appendix C – Thermal action according to EN 1991-1-2

The Eurocode (EN 1991-1-2 [2]) specifies how to predict temperature distribution from a localized fire in e.g. large compartments. In this section we show how this engineering approach is done for the experiments that are conducted here. The temperature distribution of the flame is specified according to the Heskestad plume equations [2].

First, height of flames are considered. It depends on burning source size and heat release rate, figure 1, and can be calculated using

$$L_f = -1.02D + 0.0148\dot{Q}^{2/5} \quad [\text{m}] \quad (\text{C1})$$

where D (m) is the flame thickness and \dot{Q} (W) the total heat release rate. The latter, can be calculated using mass loss rate, the heat of combustion for the evaporated gases, ΔH_c , and the combustion efficiency, χ .

$$\dot{Q} = \dot{m}\Delta H_c \cdot \chi \quad (\text{C2})$$

where the mass burning rate \dot{m} has been taking from experimental data and ΔH_c from Refs [8, 9]. The combustion efficiency is to be estimated but is rarely lower than $\chi = 0.7$ even for sooty flames as those from heptane and diesel.

The flame temperature is dependent on the convective part of the heat release rate, \dot{Q}_c i.e. what is not radiated away or left in incomplete combustion. As default this value is set to 80 % of the heat release rate. In order to allow for different interpretations of the Eurocode we make two different assumptions of the convective heat release rate. One conservative assumption is to assume that it is simply 80 % of the chemical heat release rate. In the other end, to underestimate the thermal impact we also consider the case when \dot{Q}_c is set to 80 % of a 70 % complete combustion.

$$\dot{Q}_c = \begin{cases} 0.8 \times \dot{m}\Delta H_c & \text{High} \\ 0.7 \times 0.8 \times \dot{m}\Delta H_c & \text{Low} \end{cases} \quad (\text{C3})$$

When the flame is not impacting the ceiling of a compartment or in case of fire in open space, the temperature $T(z)$ in the plume along the symmetrical vertical flame axis is given by:

$$T(z) = 20 + 0.25\dot{Q}_c^{2/3}(z - z_0)^{-5/3} \leq 900 \quad [^\circ\text{C}] \quad (\text{C4})$$

$$z_0 = -1.02D + 0.00524\dot{Q}^{2/5} \quad [\text{m}] \quad (\text{C5})$$

where z_0 is the virtual origin. There is no equation in the Eurocode for $T_{(z)} > 900$. In order not to make too conservative assumptions we therefore assume that temperature remains constant at 900 °C below that height where equation (C4) is valid.

On the fire exposed surfaces the net heat flux per unit surface area is determined according to the Eurocode as:

$$\dot{q}_{net} = \Phi \varepsilon_s \varepsilon_{fl} \cdot \sigma (T_r^4 - T_s^4) + h_c (T_g - T_s) \quad (C6)$$

Where the flame emissivity, ε_{fl} , should be set to 1, surface emissivity ε_s to 0.8 and h_c to 25 W/m²K. In our case, the configuration/view factor, Φ , can be set to unity. Equation (C6) is different from equation (4) in that both the flame emissivity and view factor are included also for the emitted radiation. Naturally, both the flame emissivity and the view factor are completely irrelevant for the emitted radiation but for thick sooty flames, where emissivities are close to one, completely engulfing the structure, it makes a marginal difference. However, for cleaner fuels, like methanol, or a fire not directly adjacent to the structure, this is not valid. In the calculations used in this report we do not use equation (C6) but correct use the correct version in equation (4).

For heights where the flames do not reach the radiative heat transfer in equation (C6) is ignored leaving only convective heat transfer to the structure. Thus, we have one estimate for low thermal impact using the low value for convective heat release rate in equation (C3) and the non-radiative gas above flame height as well as one estimate for higher thermal impact using the high value of equation (C3) and fully radiative gas. Thus, our intention is not to make a conservative estimation but to interpret the Eurocode such that the thermal exposure is as small as possible.

The steel is considered as a lumped heat capacity and we use a one-dimensional model for the heat absorption. The final expression for the steel/surface temperature increase at time step i , with a duration of Δt , can, according to EN 1991-1-2, be expressed as:

$$T_s^{i+1} = T_s^i + \frac{\dot{q}_{net}^i \cdot SF \cdot \Delta t}{\rho c} \quad (C7)$$

where ρ is density, c specific heat and the section factor, SF =cross sectional area/volume for a column section.

Appendix D –The Adiabatic Surface Temperature (AST) and plate thermometers

In most fire scenarios the radiation temperature may be either much higher or lower than the surrounding gas temperature. The adiabatic surface temperature (AST) is defined as the temperature of a surface which cannot absorb or lose heat to the environment. It is the highest temperature a specific¹ surface can obtain from a given fire. Hence, it can be obtained by solving the equation:

$$0 = \epsilon_s \sigma (T_r^4 - T_{AST}^4) + h_c (T_g - T_{AST}) \quad (D1)$$

where T_r is defined through the incident radiation.

$$\dot{q}''_{inc} = \sigma T_r^4 \quad (D2)$$

Knowledge of AST enables one to calculate the heat exposure to a surface with only one effective temperature for the fire, including both gas- and radiation temperatures, view angle and flame emissivity through the following equation [15]:

$$\dot{q}''_{tot} = \epsilon_s \sigma (T_{AST}^4 - T_s^4) + h_c (T_{AST} - T_s) \quad (D3)$$

Thus, measuring AST would give us sufficient information of the heat transfer without the detailed knowledge specified above. Measuring AST exactly is difficult but a close approximation is achieved with the use of plate thermometers (PT), originally invented to measure and control temperature in fire resistance furnaces. The PT is insulated (low losses to backside), large (convective heat transfer similar to structural surfaces) and has one exposed side (it “sees” the same thing as a structural surface). Figure 1a shows a standard plate thermometer according to ISO 834. It is made of a shielded thermocouple welded to the centre of a 0.7 mm thick metal plate which is insulated on its back side. The exposed front face is 100 mm by 100 mm. On the back side of the metal plate there is a 10 mm thick insulation pad. For this experiment special types of PT with 20 mm thick insulation pad was designed, as indicated in Figure D1 below.



Figure D1. Left: The standard PT according to ISO 834 and EN 1363-1 as mounted just outside the column. Right: Specially designed PT with extra insulation and curved surface for embedded mounting in the column.

¹ The AST for a surface given a certain fire situation is determined by one parameter of the surface. This is the ratio of surface emissivity and convective heat transfer coefficient, ϵ_s/h_c .

The temperature measured by PT is close to the AST. However, there are some differences between them due to the response time and the heat conduction loss of the PT. The correction that is required has been analysed both experimentally and through finite element analysis [15]. A simple model for the heat balance at the exposed surface of a PT is written as:

$$\epsilon(\dot{q}_{inc}'' - \sigma T_{PT}^4) + h_c(T_g - T_{PT}) + K(T_g - T_{PT}) = C \frac{dT_{PT}}{dt} \quad (D4)$$

The correction parameters for thermal loss (K) and thermal storage (C) should be set to $K=8 \text{ W/m}^2\text{K}$ and $C=4200 \text{ J/m}^2\text{K}$ for the standard PT [15].

From this relation we yield the AST from the consecutive PT measurements through a numerical procedure where the corresponding AST are recursively determined (detailed description of how this relation is obtained is given in Ref. [14]):

$$T_{AST}^{i+1} = T_{PT}^i + \frac{C \frac{T_{PT}^{i+1} - T_{PT}^i}{\Delta t} - K(T_g^i - T_{PT}^i)}{\epsilon\sigma((T_{AST}^i)^2 + (T_{PT}^i)^2)(T_{AST}^i + T_{PT}^i) + h_c} \quad (D5)$$

where Δt is the time step between consecutive recordings.

Appendix E –The effect of internal heat transfer

The FEM model of the column assumes a square section with outer surfaces subject to convective and radiant heat transfer boundaries using the AST calculated from PT measurements [14]. This approach does not capture the temperature evolution in the different positions around the column as seen in figure E1 below. The FEM results mostly overestimate the temperature in position 1 (the most exposed position) and underestimates it in position 3.

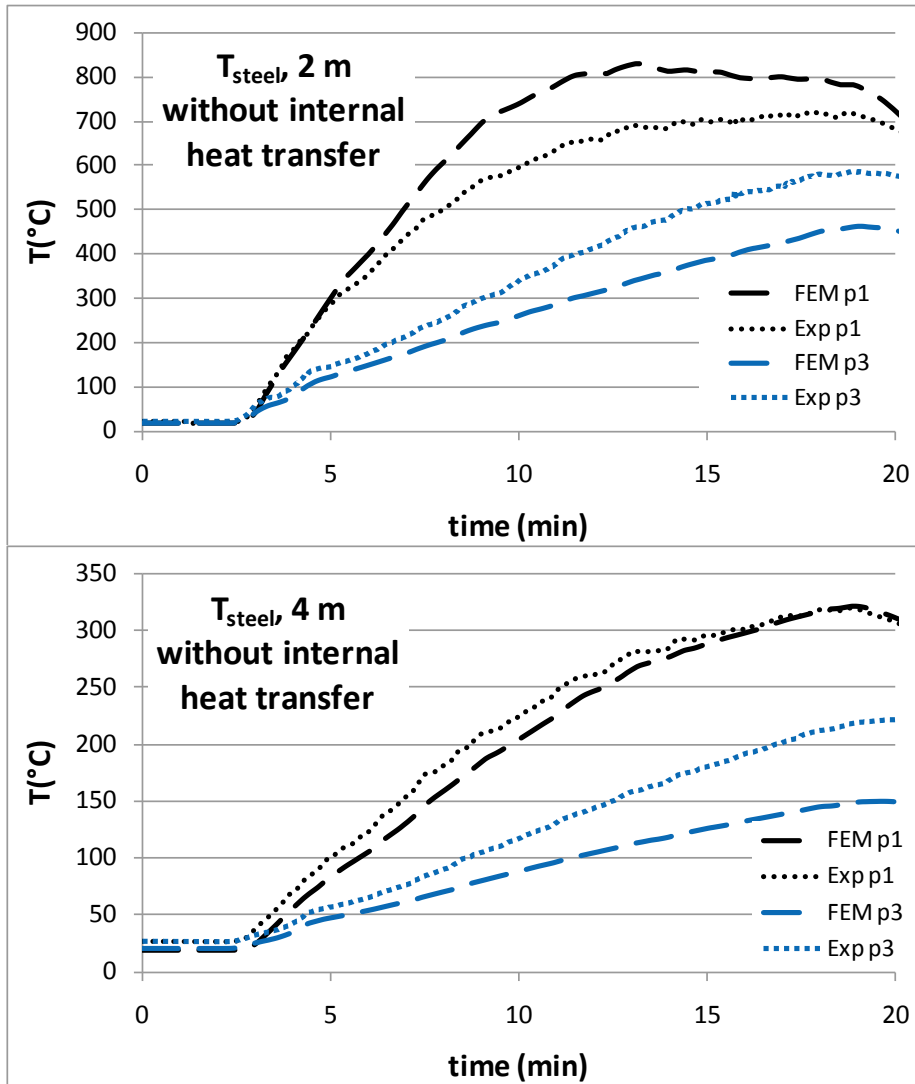


Figure E1. Steel temperatures of the column in position 1 and 3 as measured in the 1.9 m diesel fire (dotted lines) and as obtained from the finite element simulation using Eq. (8) as boundary condition (solid lines). The FEM model does not take surface-to-surface radiation within the column into account. Upper: 2 m along the column. Lower: 4 m along the column.

Taking the internal radiant heat exchange on the inner surfaces of the column, together with a small convective boundary condition of $1\text{ W/m}^2\text{K}$ the differences between the positions decreases as also seen in the experiments, see figure E2.

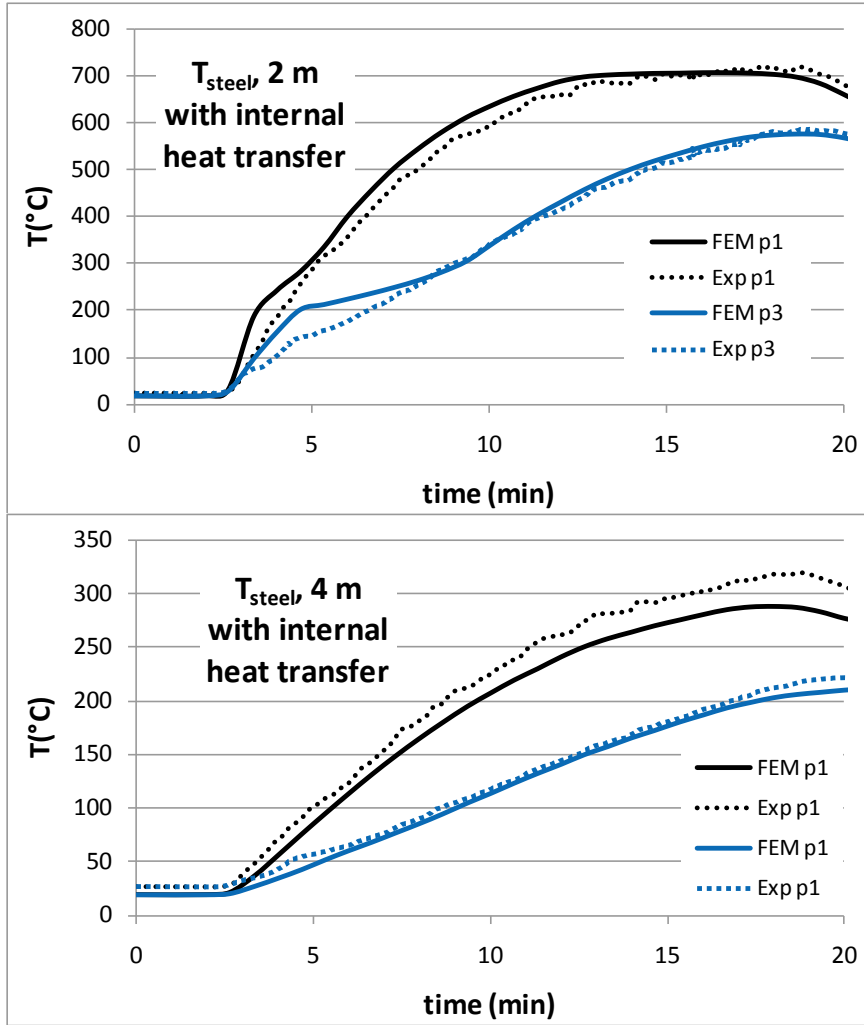
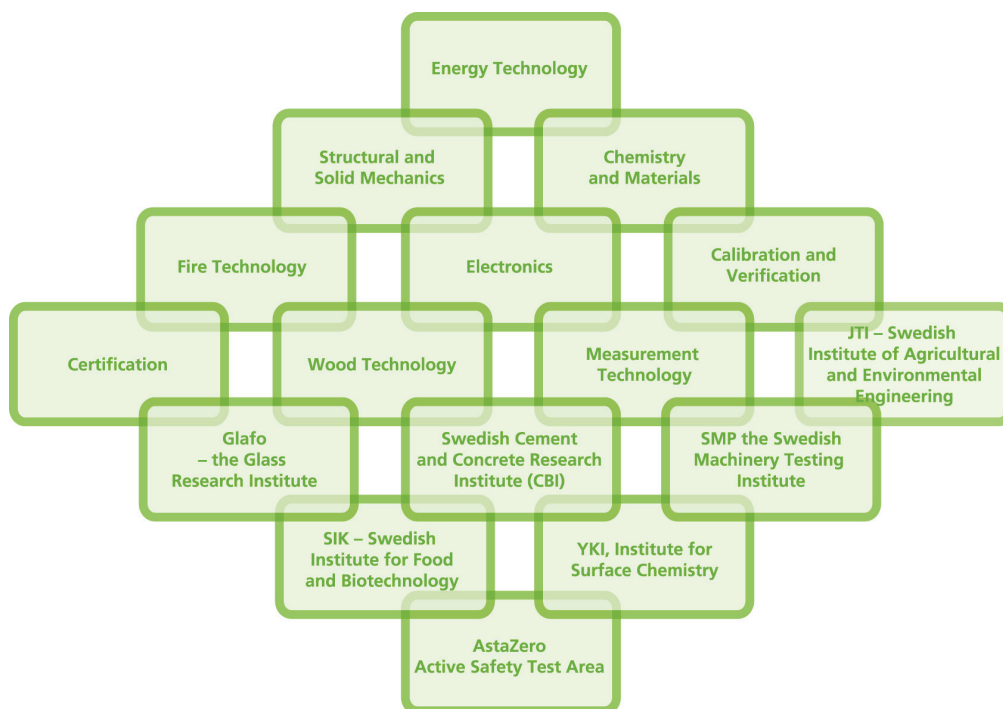


Figure E2. (Same as figure 12) Steel temperatures of the column in position 1 and 3 as measured in the 1.9 m diesel fire (dotted lines) and as obtained from the finite element simulation using Eq. (8) as boundary condition (solid lines). Internal heat transfer within the column is also taken into account. Upper: 2 m along the column. Lower: 4 m along the column.

SP Technical Research Institute of Sweden

Our work is concentrated on innovation and the development of value-adding technology. Using Sweden's most extensive and advanced resources for technical evaluation, measurement technology, research and development, we make an important contribution to the competitiveness and sustainable development of industry. Research is carried out in close conjunction with universities and institutes of technology, to the benefit of a customer base of about 10000 organisations, ranging from start-up companies developing new technologies or new ideas to international groups.



SP Technical Research Institute of Sweden

Box 857, SE-501 15 BORÅS, SWEDEN

Telephone: +46 10 516 50 00, Telefax: +46 33 13 55 02

E-mail: info@sp.se, Internet: www.sp.se

www.sp.se

Fire Technology

SP Report 2012:04

ISBN 978-91-87017-21-6

ISSN 0284-5172

More information about publications published by SP: www.sp.se/publ